

# Fast Fabrication of Multilevel Phase Plates Used for Laser Beam Correction

Roman Zakoldaev\*, Galina Kostyuk, Vladimir Rymkevich, Vladislav Koval, Maksim Sergeev, Vadim Veiko, Evgeny Yakovlev, Aleksandr Sivers

*ITMO University, Kronverkskiy pr., 49, 197101, Saint-Petersburg, Russia.*

*\*E-mail: zakoldaev@gmail.com*

Local spatial and temporal control of laser-induced microplasma (LIMP) allows to form a microrelief on fused silica plates for the fabrication of multilevel phase elements. In this work we suggested the optimal way for precision depth variation (up to 50 nm) of the microrelief (0.05 - 15  $\mu\text{m}$ ) on fused silica surface. New software and hardware were developed for the automation of optical phase elements calculation and its fabrication by LIMP. A few types of multilevel random phase plates were experimentally realized. The fabricated elements were successfully tested in the optical scheme for the correction of the highly coherent laser beam. The comparative analysis of binary and discrete phase plates was accomplished.

DOI: 10.2961/jlmn.2017.03.0018

**Keywords:** Laser plasma; fused silica; carbon; microprocessing; phase plate; beam homogenization.

## 1. Introduction

The trends of laser micro- and nano-fabrication technique development are connected with the high quality and precision of material processing. One of the key parameters of laser processing is the uniform energy distribution across the beam section in the waist plane [1]. The efficient solution of this problem is the using of beam-smoothing methods based on diffraction optical theory [2,3]. Different types of beam-smoothing optical elements were proposed, produced and tested [4-7]. The specific case of such diffraction optical elements are random phase plates (RPP) which attract universal attention [1,8-10]. Such kind of elements allowed to smooth the initial laser beam with high diffraction efficiency combined with low optical losses [11,12]. The RPP represents a glass plate with etched binary microrelief on the surface. In elementary case, the relief includes a set of squares with depth sufficient for  $\pi$  radian phase shift of used laser radiation [13]. One of the most suitable material for RPP is fused silica. This material possesses minimal radiation absorption in a wide range of wavelengths as well as high optical and thermal endurance, mechanical, chemical and electrical strength, etc. [14]. At the same time, it is a difficult task to modify or process of fused silica. One of the most common method of diffractive optical elements formation on fused silica is photolithography, but its main shortcomings are long duration of production and high cost [15,16]. That is why despite its high precision of microrelief formation, photolithography is not particularly suitable for fast and cost-effective prototyping of diffractive optical elements. The other popular technology for diffractive optical elements processing is laser thermochemical writing, which is a much simpler, but needs the set of intermediate stages as cleaning, surface coating, laser light exposure, cleaning, drying [17-19]. The alternative to these technics can become direct writing by laser

induced micro plasma (LIMP). All methods based on LIMP imply by laser erosion plasma generation at the interface between targets absorbing laser radiation (fluids [20,21], thin films [22,23] or bulk metal [24,25] and graphite [26,27]) and a processed optical material. To find out a competitiveness method among the others it is important to connect the laser fluence and plasma properties with depth sizes and roughness of formed relief.

In this work, we optimized LIMP method and established its possibilities relative to the formed microrelief (minimal depth, depth range and roughness). The operational test of LIMP method was carried out fabrication of RPPs. The comparative analysis of binary and discrete RPP used as homogenizers of He-Ne laser radiation was also provided in this work.

## 2. Laser-induced microplasma

The LIMP in this paper is considered as a special condition for erosion plasma existing. It exists when there is complete contact (comparable to the roughness of the materials) between the glass and a target. It calls as a confinement mode, involving to create a special quasiisohoric conditions for plasma evolution, characterized with the high pressure (about 1 GPa) at the interface [28-30]. Controlling the parameters (energy, living time and localization) of such plasma is the way for high precision transparent materials machining [31]. The experimental setup was described in [28-30] and its principle view is shown in Fig. 1 and includes two steps. Focused laser beam comes through the glass plate and highly absorbs by carbon target. Microplasma appears in the contact and softens and removes material from the glass surface (Fig. 1a). The scanning of laser beam across the area of micromachining allows us to achieve the microrelief with a predetermined geometry on glass surface. After the microrelief formation,

the back side of glass plate is covered by carbon particles, which are removed by wet laser cleaning using the same experimental setup (Fig. 1, b).

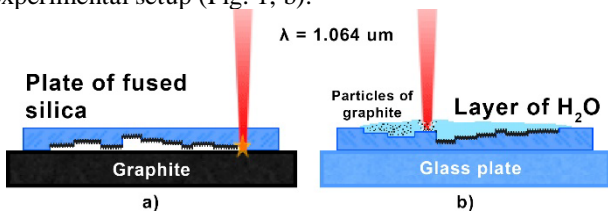


**Fig. 1** Schematic image of LIMP method: laser-induced plasma action on glass (a); laser wet cleaning (b)

The choice of the graphite-based target allows to achieve high efficiency while laser energy transformation into the carbon plasma with high temperature  $\sim 10^4$  °C, relatively high life-time (about 20  $\mu$ s) and with sufficient concentration of ions. With regard to the task of glass micromachining, it becomes clear that for the optimal use of microplasma, the following factors (which are conducted to build an experimental laser setup) should be taken into account:

1. The plasma should have the character of a pulse-periodic energy source, which corresponds with laser radiation regime and have just a desirable mode at pulse repetition  $f = 50$  kHz (at pointed lifetime);

2. Graphite target has a high absorbance, which does not depend on the wavelength of incident radiation. Thus, this allows to use lasers with any required wavelength, for which the glass is transparent.

3. The effectiveness of the energy transfer to a LIMP from laser beam energy also depends on the pulse duration, because the shorter pulse duration leads to the less thermal losses into target. Actually, at pulse duration about  $\tau = 10$  ns the thermal losses for graphite target is about 3-5 % [32].

4. The source of laser radiation must have sufficient energy to provide the required power density  $q \sim 10^8$  W/cm<sup>2</sup> (at pointed frequency, pulse duration and with typical spot size  $d \sim 50$   $\mu$ m), which should exceed the threshold for LIMP excitation. Thus, the radiation energy of the laser source must be equal to  $E = q \cdot \tau \cdot \pi d^2 / 4 \sim 0.1$  mJ and average power  $P_{avg} = E \cdot f \sim 5$  W.

Comparison of these requirements with the parameters of existing lasers led us to the conclusion that the optimal laser source for excitation of the LIMP is a pulsed ytterbium fiber laser, which is commercially available, has high efficiency and reliability. The energy efficiency of the LIMP induced by of a pulsed nanosecond fiber laser irradiation of a graphite target is actually more than 90%.

### 2.1 The possibilities of LIMP method

The formation of RPPs was carried out on the experimental setup (Fig. 2) which includes pulse Yb doped fiber laser (1) with  $\lambda = 1.07$   $\mu$ m wavelength, average power 20 W, pulse duration  $\tau = 4 - 200$  ns, pulse frequency  $\nu = 1 - 100$  kHz. The coordinate galvanometric scanning device (2) was based on drivers G325DT «GSI Lumonics». Telecentric lens (3) with focal length 210 mm and machined area 100x100 mm created laser beam waist of  $d = 50$   $\mu$ m. The fused silica plate (10x10x1 mm) (4) was placed in a

full contact with the carbon plate (5). The computer (6) was used to control the scanning system and laser source.

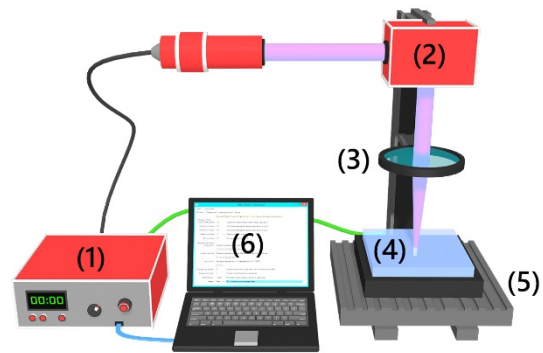


**Fig. 2** Experimental setup for the formation of RPP: 1 – Yb doped fiber laser, 2 – galvanometric scanning device, 3 – telecentric lens; 4 – fused silica; 5 – carbon target; 6 – computer

The creation of the RPP on fused silica by LIMP method required to determine relationship between the depth of the microrelief and its formation parameters. In case of LIMP method the depth of formed relief is strongly determined by laser processing parameters, transparent medium and the target properties. As a result, the determination of analytical relationship for calculation of microrelief depth is a quite complicated task. In such situation the most expedient method seems to form the database which contains relationship between the depth values and laser treatment parameters of fused silica.

In the simplest case the database of depths represents array of elementary cells each of which consists of a set of scanning tracks with overlap 90 %. Each cell contains information about microrelief depth and treatment parameters. Taking into account the fact that experimental setup allows the user to change processing parameters as radiation power, pulse repetition rate and beam scanning speed, it was decided to position cells recorded on fused silica surface in the form of two dimensional array, and title that as a depth map. In the recorded depth map the radiation power varied growing from left to right. In vertical direction each cell had its own pulse frequency and a beam scanning speed. The variable processing parameters such as pulse duration and glass material were added to the database separately. The formed depth map was investigated using profilometer Hommelwerke T-8000 (Fig. 3).

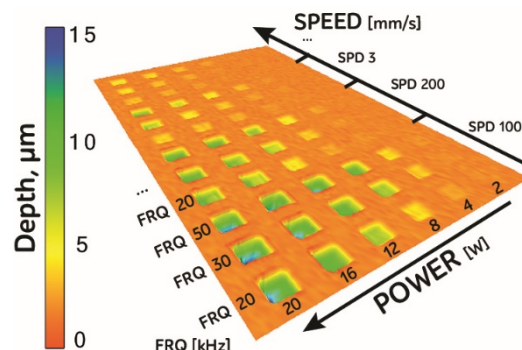


**Fig. 3** Measured 3D profile of a depth map formed on fused silica by LIMP

The obtained experimental data was collected in a single database in automatic mode using our own software «Profiles Manager». Typical depth map consists of 2400 elementary cells. The obtained cells were of different quality and depths, it was also decided to investigate statistically the depths of formed cells, which have been formed without defects. The dependence of the depth of the formed microrelief on the power density of laser radiation is presented in the diagram (Fig. 4).

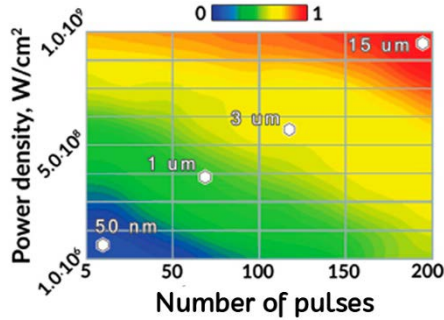


**Fig. 4** Experimentally achieved relief depth diagram: dependence of cell depth on power density and number of laser pulses

The experimental result presents that the depth of microrelief depends linearly on the power density. Having searched through different processing parameters, as a result changing power density and number of pulses, the minimal depth of the formed microrelief was equal to 50 nm at the minimal achieved depth step equal to 50 nm. The roughness of initial glass surface equal to  $R_a = 0.03 \mu\text{m}$ , while the formed cells roughness closest to initial and varied from 0.035 to 0.04  $\mu\text{m}$ .

### 3. Design, fabrication and testing of phase plates

As homogenizers of low coherent ( $l_c \sim 10^{-2}$  m and  $t_c \sim 10^{-10}$  s) laser radiation sources the binary random phase plates (BRPP) are often used [33,34] (Fig. 5a) each element of them facilitate the 0 or  $\pi$  phase shift in laser beam local area which subsequently make interference in the focal plane of the collective lens. The depth of separate element facilitating  $\pi$  phase shift is determined by expression (1):

$$h = \frac{\lambda}{2(n-1)}, (1)$$

where  $\lambda$  – wavelength of used laser source,  $n$  - refractive index of machining material.

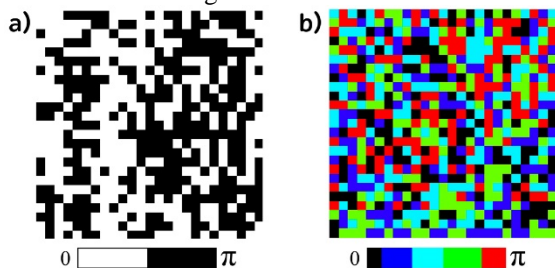


**Fig. 5** Template of binary (a) and discrete (b) random phase plates generated by our own software

The BRPP is not suitable to transform the intensity distribution of highly coherent radiation ( $l_c \sim 3 \cdot 10^5$  m and  $t_c \sim 10^{-3}$  s). For such purpose the complicated multicomponent elements with continuous relief should be designed and

fabricated [1,35]. From the other hand, the modification of binary template into a discrete (with discretely varying in depth) can suit for highly coherent laser radiation hominization. The increase of the number of depth step (which enables phase shift from 0 to  $\pi$ ) will result in the increase of the number of overlapping interference patterns in the lens focal plane. An important requirement when designing a DRPP's template is the presence of the same number of cells with different phase shifts (Fig. 5b). In this case, it will be possible to obtain a uniform intensity profile. This is due to the interference of elementary beams with one phase between them. The presence of bigger set of different phase shifts will allow to obtain the same set of interference patterns with different periods that will overlap and form a quasi-uniform intensity distribution [36]. In the process of such RPP fabrication, the deviation of the cell depth from the projected one is possible, which will insignificantly reduce the intensity of the interference speckle pattern.

The obtained depth map data allowed us to fabricate both types of RPP (according to the templates presented in Fig. 5), whose application is aimed at homogenization of the laser beam. The size of each cell was equal to 200  $\mu\text{m}$ . Our self-made software «LIBBH Pipeline» allows us to calculate and generate the template of RPPs for its fabrication of glass plate by LIMP.

First of all, the BRPP was fabricated. It was suggested to test phase plates with He-Ne laser. That is why according to the formula (1) for the fused silica ( $n = 1.457$ ) the depth of elementary cell facilitating phase shift of  $\pi$  should be 0.69  $\mu\text{m}$ . After fabrication process, the topology of the element was investigated to estimate the depth of cells and the stability of their formation (Fig. 6). The obtained profile confirmed reproducibility of the formed cells with certain depth using the regimes found earlier by the depth map.

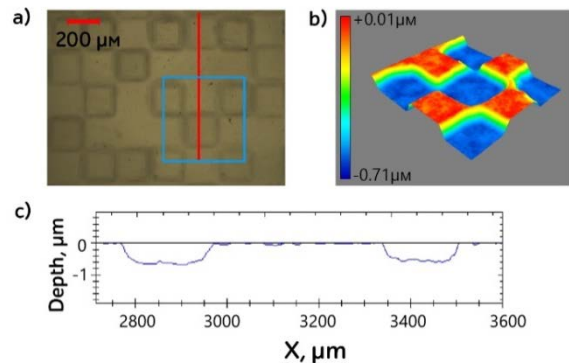


**Fig. 6** Investigation of fabricated BRPP: optical image (a), surface topology (b) and profile (c)

The DRPP was fabricated on fused silica for the same wavelength as the binary plate. The number of cells of different depth was limited to five values (0 – skipped cell,  $\pi/4$  ( $h \sim 0.17 \mu\text{m}$ ),  $\pi/2$  ( $h \sim 0.35 \mu\text{m}$ ),  $3\pi/4$  ( $h \sim 0.53 \mu\text{m}$ ) and  $\pi$  ( $h \sim 0.7 \mu\text{m}$ ). The obtained sample was investigated using microscope in reflected light (Fig. 7a). The profile investigation of the DRPP surface demonstrated good correlation with the required geometry (Fig. 7b, c).

Subsequently both homogenizers underwent comparative analysis. The investigation of phase plates as laser radiation homogenizers was performed on the experimental setup with He-Ne laser (Fig. 8) where laser radiation beam

with the wavelength of  $\lambda = 0.633 \mu\text{m}$  was widened by the telescopic system with magnification of  $\times 4$ . A thin needle (with diameter of 1 mm) was placed behind the telescopic system. The needle was used to distort the intensity distribution over the beam cross-section. The RPP was placed after telescopic system, then radiation passed through the mounted RPP and was focused by collecting lens on the matrix of CCD camera.

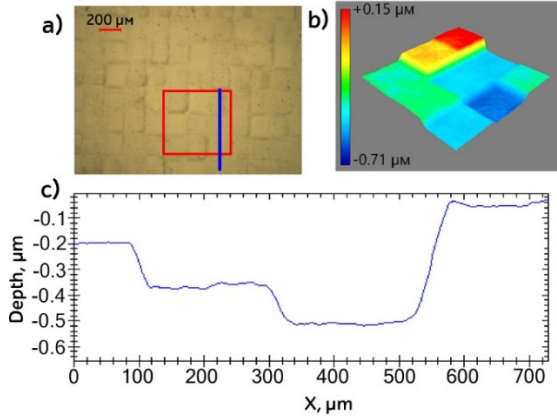


**Fig. 7** Fabricated DRPP: optical image (a), surface topography (b) and profile (c)

The testing of RPPs was accomplished in the following way. The distorted intensity distribution of the He-Ne laser was registered close to the lens focal plane (Fig. 9a). Afterwards the RPP was set into the setup before the collective lens and registration was performed one more time (fig. 9b). The BRPP usage caused the appearance of diffraction pattern (or speckle pattern) in the focal plane of the collective lens and the incident beam becomes homogeneous and wider size of  $\sim 4.5 \text{ mm}$ . Applying super Gaussian [37] fit the deviation of the speckle pattern was equal to 25 %.

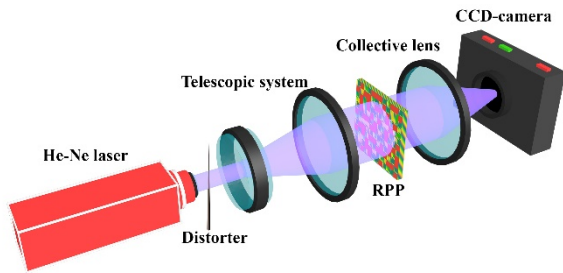


**Fig. 8** The experimental setup for RPP testing

In case of DRPP, it can be seen more intensity redistribution in the diffraction pattern relative to the central maximum compared with BRPP results. The application of DRPP appeared to be more efficient than BRPP for the correction of the distorted beam diffraction pattern. It is evident from Fig. 9c that the level of most intensity peaks in the profile has the same intensity and the average intensity modulation of the diffraction pattern is equal to  $\sim 9\%$ .

In addition, the optical losses introduced by the RPP were estimated in the scheme (Fig. 8) by comparing the optical power in the measurement plane without and using RPP. The measurements were carried out using Gentec Solo-2M equipped with a pyroelectric power meter. The transmission losses in case of BRPP were  $\sim 10\%$  and DRPP

$\sim 12\%$ . The resulting losses are related to both Fresnel reflection and diffraction by microstructure.

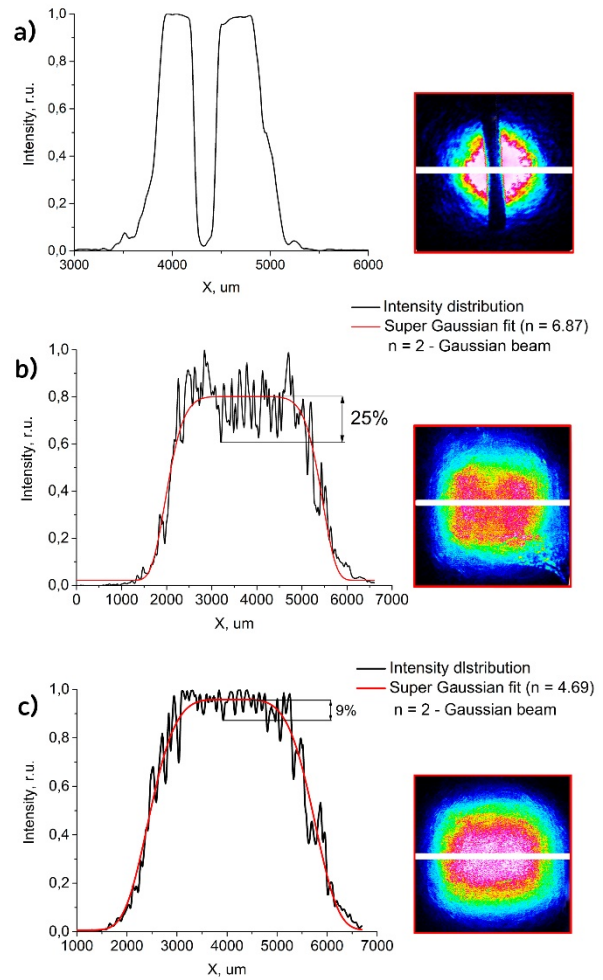


**Fig. 9** Intensity distribution without (a) and with using BRPP (b) and DRPP (c)

#### 4. Conclusion

The LIMP method used for microprocessing of fused silica was supplemented with opportunity to control the depth of the formed microrelief. The software for the automatization of this process was developed. On the bases of process automatization the databases connecting main parameters of laser radiation and the depth of formed cells were compiled. This made possible to record random phase plates with required discrete and binary structure.

As a result of executed research it was determined that the utilization of random phase plate having discrete structure is more preferable to obtain uniform intensity distribution in comparison with binary random phase plate. In particular, the DRPP with 5 different phase shifts for elementary cell of  $200 \mu\text{m}$  size used in present work allowed us to obtain profile standard deviation from uniform intensity distribution less than 10%. It seems to us that the possible reducing the deviation of the intensity distribution could be the creation of a DRPP with a large number of steps in depth.

The control of the formed relief depth plays the key role in the creation of different diffractive optical element. That is why performed improvement of LIMP method in

the process of RPPs formation which requires high precision of the microrelief depth became the first step to the solution of this urgent task. It will allow using this method for fabrication of more complex and multilevel diffractive optical element.

### Acknowledgments

The reported study was financially supported by the Ministry of Education and Science of the Russian Federation, research agreement №14.587.21.0037 (RFMEFI58717X0037).

### References

- [1] C. Yang, H. Yan, J. Wang, R. Zhang: *Opt. Exp.* 21, (2013) 11171.
- [2] D. Veron, H. Ayril, C. Gouedard, D. Husson, J. Lauriou, O. Martin, B. Meyer, M. Rostaing, C. Sauteret: *Opt. Commun.* 65, (1988) 42.
- [3] C.J. Zapata-Rodríguez, M.T. Caballero: *Opt. Lett.* 32, (2007) 2472.
- [4] Y. Kato, K. Mima, N. Miyanaga, S. Arinaga, Y. Kitagawa, M. Nakatsuka, C. Yamanaka: *Phys. Rev. Lett.* 53, (1984) 1057.
- [5] S. Dixit, K. Nugent, J. Lawson, K. Manes, H. Powell: *Opt. Lett.* 19, (1994) 417.
- [6] J.A. Marozas, *J. Opt. Soc. Am. A*: 24, (2007) 74.
- [7] K.L. Wlodarczyk, E. Mendez, H.J. Baker, R. McBride, D.R. Hall: *Appl. Opt.* 49, (2010) 1997.
- [8] C. Lewis, I. Weaver, L. Doyle, G. Martin, T. Morrow, D. Pepler, C. Danson, I. Ross: *Rev. Sci. Instrum.* 70, (1999) 2116.
- [9] G. Kopitkovas, T. Lippert, C. David, S. Canulescu, A. Wokaun, J. Gobrecht: *J. Photochem. Photob. A* 166, (2004) 135.
- [10] X. Jiang, J. Li, R. Wu, Z. Zhu, S. Zhou, Z. Lin, J. Opt. Soc. Am. A 30, (2013) 2162.
- [11] J. Neauport, X. Ribeyre, J. Daurios, D. Valla, M. Lavergne, V. Beau, L. Videau: *Appl. Opt.* 42, (2003) 2377.
- [12] C. Yang, R. Zhang, Q. Xu, P. Ma; *Appl. Opt.* 47, (2008) 1465.
- [13] S. Dixit, I.M. Thomas, B.W. Woods, A. Morgan, M. Hennesian, P. Wegner, H. Powell: *Appl. Opt.* 32, (1993) 2543.
- [14] N.P. Bansal, R.H. Doremus: "Handbook of glass properties" ( Elsevier, USA, 2013) p. 680.
- [15] J. Baglin: *Appl. Surf. Sci.* 258, (2012) 4103.
- [16] E. Becker, W. Ehrfeld, P. Hagemann, A. Maner, D. Münchmeyer: *Microel. Eng.* 4, (1986) 35.
- [17] V. Veiko, E. Shakhno, D. Sinev: *Opt. Quant. Electron.* 48, (2016) 1.
- [18] V.P. Veiko, V.I. Konov: "Fundamentals of Laser-Assisted Micro-and Nanotechnologies" (Springer, the Netherlands, 2014) p. 322.
- [19] V. Veiko, E. Shakhno, A. Poleshchuk, V. Korolkov, V. Matyzhonok: *J. Laser Micro/Nanoeng.* 3, (2008) 201.
- [20] H. Niino, Y. Kawaguchi, T. Sato, A. Narazaki, T. Gumpenberger, R. Kurosaki: *J. Laser Micro/Nanoeng* 1, (2006) 39.
- [21] G. Kopitkovas, T. Lippert, C. David, A. Wokaun, J. Gobrecht: *Microel. Eng.* 67, (2003) 438.
- [22] B. Hopp, T. Smausz, C. Vass, G. Szabó, R. Böhme, D. Hirsch, K. Zimmer: *Appl. Phys. A* 94, (2009) 899.
- [23] B. Hopp, T. Smausz, M. Bereznai: *Appl. Phys. A* 87, (2007) 77.
- [24] Y. Hanada, K. Sugioka, I. Miyamoto, K. Midorikawa: *Appl. Surf. Sci.* 248, (2005) 276.
- [25] Y. Hanada, K. Sugioka, K. Midorikawa: *VI Int. Soc. for Opt. Photon, USA*, (2006) p. 626111.
- [26] R. Zakoldaev, M. Sergeev, G. Kostyuk, V. Veiko: *J. Laser Micro/Nanoeng.* 10, (2015) 15.
- [27] S. Xu, B. Liu, C. Pan, L. Ren, B. Tang, Q. Hu, L. Jiang: *J. Mat. Proc. Tech.* 247, (2017) 204.
- [28] G. Kostyuk, R. Zakoldaev, V. Koval, M. Sergeev, V. Rymkevich: *Opt. Lasers in Engin.* 92, (2017) 63.
- [29] G. Kostyuk, R. Zakoldaev, M. Sergeev, V. Veiko: *Opt. Quant. Electr.* 48, (2016) 1.
- [30] G. Kostyuk, M. Sergeev, R. Zakoldaev, E. Yakovlev: *Opt. Lasers Eng.* 68, (2015) 16.
- [31] Lu, X., Jiang, F., Lei, T. P., Zhou, R., Zhang, C., Zheng, G., Chen, Z.: *Micromachines*, 8, (2017) 0300.
- [32] V. Veiko, S. Volkov, R. Zakoldaev, M. Sergeev, A. Samokhvalov, G. Kostyuk, K. Milyaev: *Quant. Electr.* 47, (2017) 842.
- [33] C.L.S. Lewis, I. Weaver, L.A. Doyle, G.W. Martin, T. Morrow, D.A. Pepler, C.N. Danson, I.N. Ross: *Rev. Sci. Instrum.* 70, (1999) 2116.
- [34] C. Kopp, L. Ravel, P. Meyrueis: *J. Opt. A* 1, (1999) 398.
- [35] M. Cumme, A. Deparnay: *Adv. Opt. Tech.* 4, (2015) 47.
- [36] D.A. Pepler, C.N. Danson, R. Bann, I.N. Ross, R. Stevenson, M. Norman, M. Desselberger, O. Willi: *OE/LASE'93 USA*, (1993) p. 76.
- [37] F.J. Decker: *AIP, USA*, (1995) p. 550.

(Received: July 8, 2017, Accepted: November 20, 2017)